Integration of a Multi-Stack Fuel Cell System in Microgrids: A Solution Based on Model Predictive Control

Antonio José Calderón [1],*[ID]**, Francisco José Vivas** [2][ID]**, Francisca Segura** [2][ID] **and José Manuel Andújar** [2][ID]

1   Department of Electrical, Electronics Engineering and Automatic, Campus Universitario, University of Extremadura, Av. de Elvas, s/n, 06006 Badajoz, Spain
2   CITES (Centro de Investigación en Tecnología, Energía y Sostenibilidad), Campus El Carmen, University of Huelva, 21071 Huelva, Spain; francisco.vivas@diesia.uhu.es (F.J.V.); francisca.segura@diesia.uhu.es (F.S.); andujar@diesia.uhu.es (J.M.A.)
*   Correspondence: ajcalde@unex.es

Abstract: This paper proposes a multi-objective model predictive control (MPC) designed for the power management of a multi-stack fuel cell (FC) system integrated into a renewable sources-based microgrid. The main advantage of MPC is the fact that it allows the current timeslot to be optimized while taking future timeslots into account. The multi-objective function solves the problem related to the power dispatch at time that includes criteria to reduce the multi-stack FC degradation, operating and maintenance costs, as well as hydrogen consumption. Regarding the scientific literature, the novelty of this paper lies in the proposal of a generalized MPC controller for a multi-stack FC that can be used independently of the number of stacks that make it up. Although all the stacks that make up the modular FC system are identical, their levels of degradation, in general, will not be. Thus, over time, each stack can present a different behavior. Therefore, the power control strategy cannot be based on an equal distribution according to the nominal power of each stack. On the contrary, the control algorithm should take advantage of the characteristics of the multi-stack FC concept, distributing operation across all the stacks regarding their capacity to produce power/energy, and optimizing the overall performance.

Keywords: PEM fuel cell; multi-stack; model predictive control; multi-objective; microgrid

1. Introduction

The beginning of a new decade is always expected as a period of new challenges and opportunities, but the period 2020–2030 has started with global problems that directly and seriously affect humanity. There are many voices that warn about current and future climate change impacts on human health, and how our societies can lessen those adverse impacts through adaptation strategies and by reducing greenhouse gas emissions [1]. In this sense, governments from different parts of the world and with different political ideology, agree on the need for a worldwide effort during this decade to offset the fossil fuel depletion and reduce the greenhouse gas emission. Then, the European Commission and the United States Department of Energy (DOE) have set their targets for 2030 in the promotion of renewable energy sources (RES), sharing up to 27% of energy from renewables [2,3]. Meanwhile, China's National Development and Reform Commission (NDRC) has set a draft policy to increase the RES target from 20% to 35% by 2030 [4]. Therefore, the global population has not only started the current decade facing a human health threat but also must end the decade by solving the challenges of climate change.

For this purpose, renewable sources-based electrical microgrids are a promising and efficient solution by integrating various distributed renewable energy sources (RES), energy storage systems (ESS), and interconnected loads that act as a single controllable entity with respect to the utility grid [5]. Among the renewable alternatives to be integrated into the microgrids, such as wind, solar, hydroelectric, and biomass, FCs has been demonstrated to be a promising solution to carry out the conversion of these renewable energy sources into hydrogen, as it can provide reliable, efficient, clean and quiet energy [6].

Given the stochasticity of most RES (e.g., solar, wind, etc.), FCs, along with energy storage systems (ESSs), can be used to mitigate the intermittency induced by stochastic RES, and they serve as an effective solution due to their reliable output power [7]. However, despite these numerous advantages, the integration of FCs into microgrids requires an exhaustive energy management system (EMS) that takes into account the low durability and high cost of FCs [8], at the time that guarantees crucial features like reliability, resiliency, and safety, more and more crucial in microgrids [9,10].

On the other hand, regarding the architecture of hybridized microgrids, most of the studies combine multiple ESSs with the aim to gather the advantages of different storage solutions [11–13]. However, despite the fact that all these researchers consider different RES and ESS into the microgrid, in all these works, the FC system is made up of a single stack. Then, A. Kamel et al. [11] proposed a system that combines photovoltaics (PVs), batteries, ultracapacitors (UCs), with a 10 kW-single stack FC to supply a load dump. Anastasiadis et al. present in [12] an optimization model in order to determine the viability and the environmental contribution of microgrids, taking into account the high penetration of FC units and RES, but all the study cases are based on 10 kW to 50 kW single stacks. Even at high power, Li et al. proposed in [13] a fuzzy logic-based EMS, and the major portion of the low-frequency power demand can be dealt with a 150 kW-single stack FC. A single-stack FC system simplifies the balance of plant (BoP) design and the power management inside the FC system, but its main disadvantage is that in case of damage or excessive losses, the entire system must be disconnected from the microgrid.

To solve this, Marx et al. announced in [14] that a multi-stack FC structure can provide more redundancy than single stack-based systems thus that the system reliability can be improved. The efficiency of multi-stack FC systems can also be increased by optimally distributing the demanded power among different stacks [15]. That is, multi-stack FCs are manufactured in standard size and can be easily combined to meet different power demands. More units can be added as the microgrid energy demand grows over time without having to redesign and reconstruct the whole plant. Then, Palma and Enjeti developed in [16] a multi-stack based fuel cell system connected to a modular DC-DC converter. Under the premise that a stack producing a higher voltage can generate more power than a stack that produces a lower voltage, the control algorithm defines the load current on each module as a function of the voltage (the least damaged modules supply more power than the deteriorated). The loop control is based on a Proportional-Integral-Derivative (PID) controller to calculate the required duty cycle for each DC-DC converter module. The reference signals are calculated by taking into account the voltage produced by each module. If one of the modules produces a voltage below the threshold level, that module is considered damaged, and the reference signals of the remaining modules are increased to compensate for the loss of that module. Despite the hardware implementation novelty, this work lacks the possibility to include optimization criteria; the control algorithm just establishes the power reference to each stack regarding the degradation of each stack.

A deeper study was carried out by García et al. in [17], where the authors detailed the influence of power-sharing methods on the efficiency of a multi-stack FC system. The power-sharing methods tested were the following. (1) Equidistribution: Split the power reference equally between the different fuel cells; (2) Daisy Chain: Distributes the power reference sequentially to the stacks; and (3) Optimization-based distribution. The power reference is shared between the different FCs to achieve the highest efficiency available at that power reference. Results show that the equidistribution method provides results close to those of a single stack FC system, while the daisy-chain distribution method

provides higher efficiency at low power outputs. The best behavior is offered by the optimization-based power-sharing method. The optimization-based method is an interesting algorithm that calculates power distribution coefficients to maximize efficiency at a given power setpoint. Results show that the efficiency of the multi-stack FC system achieves the maximum efficiency available throughout most of the power range. However, despite these interesting results, the work is developed under two severe constraints: (1) The behavior of all the stacks is supposed similar, and (2) the aging and operation condition dependence is not considered. These assumptions go against fuel cell fundamentals: FC degradation is highly dependent on the operating conditions, and fault diagnosis is crucial to keep the FC system operating safely and efficiently, and to mitigate performance degradation [18].

In this sense, Herr et al. proposed in [19] a mixed-integer linear programming (MILP) management strategy for multi-stack FC systems to extend its lifespan in a prognostics and health management (PHM) framework. The strategy consists of selecting at each time which stacks must run and which output power has to be chosen for each of them to satisfy a load demand as long as possible. Multi-stack FC system lifespan depends not only on each stack's lifespan but also on both the schedule and the operating conditions that define the contribution of each stack over time.

As can be seen, advanced control techniques are highly recommended for optimization problems under constraints in a prediction horizon. Then, the proposal developed in [19] can be improved by applying predictive control techniques that take into account not only technical but also economic criteria. That is, a power-sharing control that takes decisions regarding not only the load supply and lifespan extension, but also looking for economic savings, is considered one of the best solutions to solve optimization problems [20].

Based on the above, this paper contributes to the control theory in multi-stack FC systems integrated into a RES-based microgrid proposing a multi-objective model predictive control (MPC) designed for the power management of a multi-stack FC system. The multi-objective function solves the problem related to the power dispatch at time that includes criteria to reduce the multi-stack FC degradation, operating and maintenance costs, as well as hydrogen consumption. The main advantage of MPC is the fact that it allows the current timeslot to be optimized while keeping future timeslots in account [21].

Regarding the scientific literature, the novelty of this paper lies in the proposal of a generalized MPC controller for a multi-stack FC, and it can be used independently of the number of stacks that make it up. Even though all the stacks that make up the modular FC system are identical, the level of degradation that each one suffers can give it different behavior. Therefore, the power control strategy cannot be based on a balanced distribution according to its nominal power. On the contrary, the control algorithm should take advantage of the characteristics of the multi-stack FC concept, distributing operation across all the stacks and optimizing the overall performance. To carry out this distribution, the control system must always know the real state of each stack to determine its real capacity to produce energy. In the revision of the scientific literature, no previous study has been found that addresses the power management of multi-stack FC systems taking into account the optimization of its performance while preserving the stacks' lifespan and reducing the hydrogen consumption with respect to a single stack-based FC system. Table 1 gathers the main features of this paper with respect to previous works found in the literature.

The paper is organized as follows, Section 2 describes all the facilities, devices, and tools software that have been used to carry out the research. Section 3 presents the MPC controller for the multi-stack FC system, and results are discussed in Section 4. Finally, in Sections 5 and 6, discussions and principal conclusions of the research are addressed.

Table 1. Comparison of the findings of the proposed paper with previous scientific works.

Reference	Fuel Cell System Configuration	Nominal Power	Power Control Algorithm	Optimization Criteria	Predictability
Authors proposal	Multi stack (3 stacks)	7.5 kW 2.5 kW/stack (expandable)	Model Predictive Control (MPC)	Provide load demand Reduce degradation Reduce hydrogen consumption Minimize O&M costs *	Yes
[11]	Single stack	10 kW	-	-	-
[12]	Single stack	10–50 kW	-	-	-
[13]	Single stack	150 kW	-	-	-
[16]	Multi stack	150 W	PID	Fault detection in stack	No
[17]	Multi stack	2.5 kW	Equi-distribution	Load demand	No
			Daisy Chain	Load demand	No
			Optimization-based distribution	Maximize efficiency	No
[19]	Multi stack (3 stacks)	1.5 kW 500 W/stack	Mixed Integer Linear Programming (MILP)	Provide load demand, Prognostics and Health Management (PHM)	Yes

* Operation and maintenance costs

2. Materials and Methods

The microgrid under study was based on the production of energy entirely obtained from renewable resources, which guaranteed the production and storage of energy with zero CO_2 emissions, Figure 1. The microgrid included different renewable energy generation systems consisting of a 15 kWp photovoltaic plant (5 kWp monocrystalline technology, 5 kWp polycrystalline technology, and 5 kWp thin-film technology), along with a hydrogen system composed by a modular fuel cell of 7.5 kWe made up of 3 stacks of 2.5 kW each, a 10 kWe alkaline electrolyzer (7 kWe for the bipolar electrolytic stack and 3 kWe for auxiliaries), and a lead-acid battery storage bank with a storage capacity of 36 kWh [22].

It is located on "La Rábida" Campus, at the University of Huelva (Huelva is located in the southwest of Spain), and according to its topology, all the generation and consumption systems were connected to an internal DC bus supported by a battery bank. The renewable generation was provided by solar radiation, which allowed the production of up to 15 kWp from PV panels. To guarantee the power balance at all times, there were 2 ESSs available. The first ESS was a 36 kWh lead-acid battery bank; the direct connection of this battery bank to the internal DC bus avoided the need for power conditioners to guarantee the regulation of the bus voltage. The second ESS was a hydrogen loop, consisting of an alkaline electrolyzer that produces 2 Nm^3/h of hydrogen under a rate load power of 10%–100% and efficiency of 85%. Additionally, a 7.5 kWe modular multi-stack FC system acted as a hydrogen consumer with an efficiency of 47%, and a compressed hydrogen storage tank of 1 Nm^3 and 30 bars (this is equivalent to 88 kWh; that is 2.4 times the energy stored in the battery bank). This hydrogen loop allowed achieving a power-to-hydrogen and hydrogen-to-power roundtrip efficiency around 40%. Finally, all the power conditioning, as well as the bidirectional power flow between the main power grid and the microgrid, were guaranteed by DC/DC and DC/AC power converters.

As has been commented in Section 1, one of the options for improving FC effectiveness, extending its lifespan, and reducing costs, were to use such stacks in a modular architecture to develop scalable power FC systems as needed [23]. Using a modular architecture to implement the FC system as a connection of independent stacks (multi-stack) aimed to meet with the power demand (with one, several, or all stacks running) while taking into account the level of stacks degradation and O&M costs. This allowed the microgrid energy management system (EMS) to control the multi-stack FC system according to technical and economic criteria, leading to optimized behavior, reducing the degradation, preserving the lifespan, and minimizing the hydrogen consumption [24].
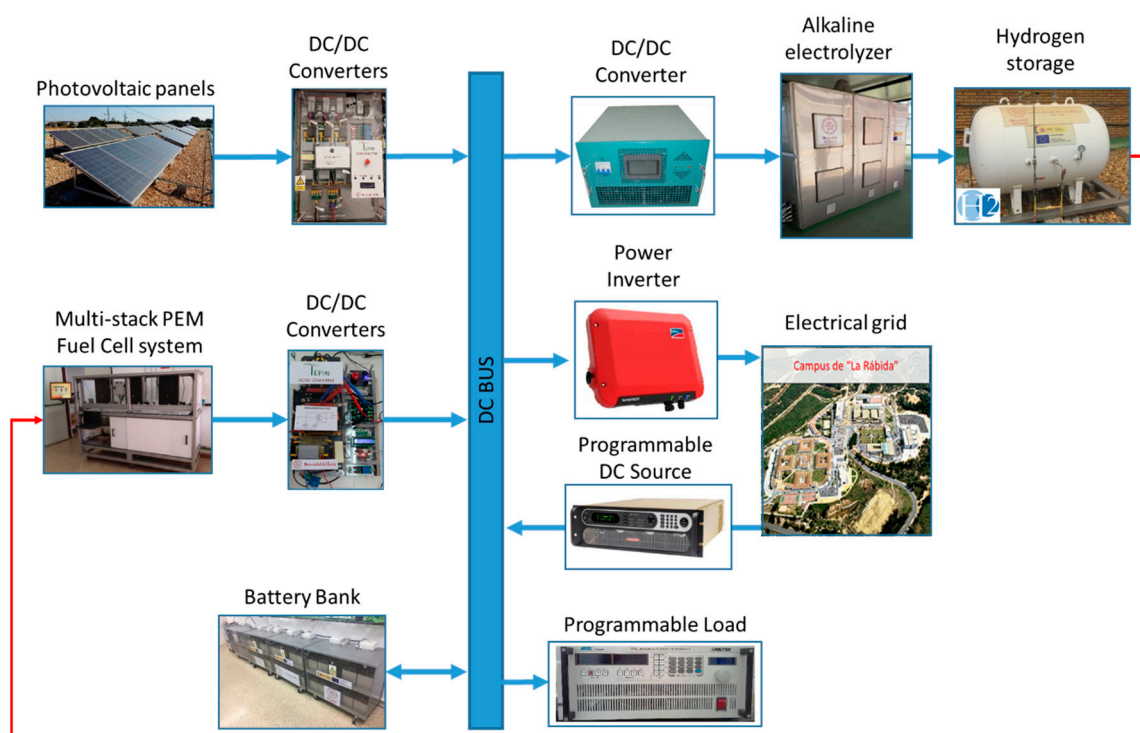
Figure 1. General microgrid architecture (University of Huelva).

An additional advantage of a multi-stack configuration was the possibility to discriminate one of them in the case of located damage or excessive losses, avoiding the disconnection of the entire FC system. These characteristics provided high flexibility and scalability, robustness, reliability, and good performance to the microgrid [19,25].

Considering *n* identical stacks (Figure 2a), our experience says that even in the beginning, when all stacks are brand new, there is a great possibility that their behaviors will be different. Of course, with time and use, the differences in the stacks' behavior will be increasingly evident. Therefore, the control strategy cannot be based on an equal distribution according to each stack nominal power. On the contrary, the controller should take advantage of the characteristics of the multi-stack FC concept, distributing operation in each stack and optimizing overall performance. That is, the input to the MPC controller will be the reference power established by the EMS, and based on technical and economic criteria, the MPC defines the setpoint of each stack. To carry out this distribution, the control system must always know the real state of each stack to determine its real capacity to produce energy. Figure 2b shows a branch of the fuel cell (stack + BoP + power electronics), and Figure 2c the complete multi-stack real fuel cell system integrated into the microgrid (see Figure 1). The stacks are based on the FCgen-1020ACS model from Ballard® (Seattle, WA, USA). It is a polymer electrolyte membrane (PEM) stack made up of a stack with 80 single planar cells in series, with an active surface of 0.0145 m^2/cell. Its current nominal power is 2.5 kW [26]. Technical characteristics are reported in Table 2.

Table 2. FCgen-1020ACS stack technical characteristics.

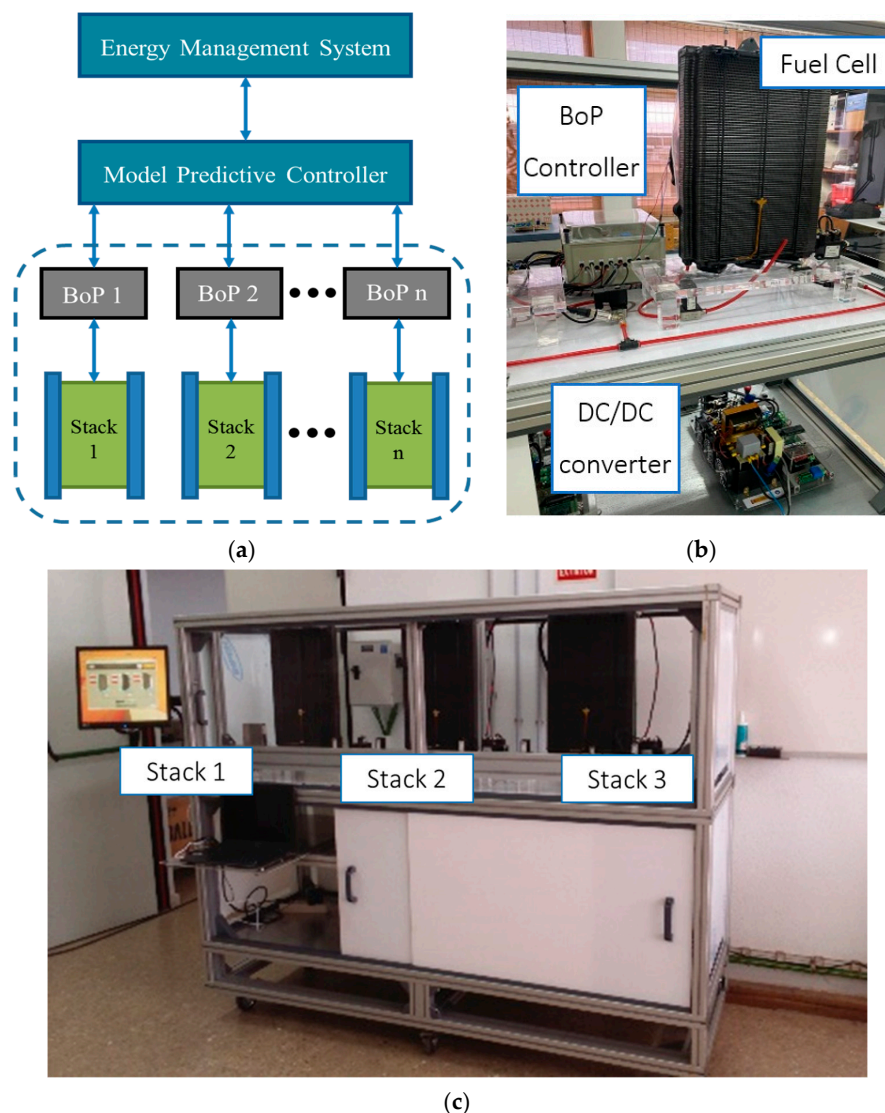| Characteristics	Value	Unit
Nominal power	2.5	kWe
Number of cells	80	units
Active area	0.0145	m^2/cell
Hydrogen consumption	1.3	Nm^3/h
Hydrogen pressure	1.36	bar

Figure 2. (**a**) Block Diagram and model predictive control (MPC) control architecture for a multi-stack fuel cell (FC) system; (**b**) detail of a single fuel cell (stack + BoP + power electronics); (**c**) detail of the real multi-stack system integrated into the microgrid.

3. Model Predictive Control (MPC) for Multi-Stack FC System

Regarding the microgrid scheme shown in Figure 1, the EMS was responsible for defining the operating point of each source. In the case of the FC system, the EMS provided the power reference that the FC system must supply to the internal bus.

Based on the advantages that a multi-stack FC system presents, the MPC controller receives the power reference (Figure 2a), and it will decide the power setpoints under a multi-objective scenario that involves both technical and economic criteria in the multi-stack FC system, that is: To guarantee the power demand, to reduce the degradation, minimize the hydrogen consumption, and secondarily to diminish the operating costs.

3.1. Generalized Model for Multi-Stack FC System with n Stacks

In a general way, MPC theory makes explicit use of the plant model to optimize its expected future behavior. Then, a suitable model of the plant allows the MPC controller to lead it to its best performance. Based on the above, the first step to carry out the controller design was to dispose of an appropriate plant model that allows predicting the future behavior of the plant.

In this section, the generalized model of the multi-stack FC system with n stacks will be depicted. The proposed model was defined as a linear parameter variant (LPV) model, which allowed defining the non-linear behavior of the multi-stack FC system as a linearized model in each sampling period [21].

3.1.1. Multi-Stack FC System Power

In accordance with the architecture under study, the predicted output power of the multi-stack FC system, P_{sys}, will be determined by the sum of the individual operating powers of each of the n stacks, P_{fc_x}, $x = 1 \ldots n$, at each sampling time k, Expression (1).

$$P_{\text{sys}}(k+1) = \sum_{x=1}^{n} P_{fc_x}(k) \tag{1}$$

3.1.2. Multi-Stack FC System Degradation

Regarding the multi-stack FC system degradation, due to the fact that its operating conditions strongly influence its lifespan [27], each stack degradation, D_{fc_x}, will be quantified in terms of its voltage drop considering the operating hours and cycles (V/h), $\Delta V_{fc\_x_{time}}$, with respect to its nominal operating conditions, $P_{fc_{N_x}}$. Voltage drop, $\Delta V_{fc\_x_{time}}$, is an experimentally calculated parameter. It quantifies the voltage drop of one cell based on the number of hours and operation cycles under nominal operating conditions [28]. For simplicity, a linear relationship among the degradation factor and the working power was assumed. This assumption was based on the experience of the authors with numerous tests and works with fuel cells with different nominal power and their operation under different working conditions. As a result of this research, it was shown that the degradation parameter normally provided by the manufacturers was not constant and depended directly on the operating current/power due to the interaction between these variables and the temperature and humidity on the membrane. Similar considerations have been obtained in scientific works such as [29,30]. The instantaneous minimization of the degradation parameter related to each stack did not guarantee the long-term optimization of the multi-stack system. The controller required the accumulated degradation value of each stack. Therefore, stack degradation, D_{fc_x} was calculated from the integral of its accumulated degradation, Expression (2).

$$D_{fc_x}(t) = D_{fc_x}(t_0) + \Delta V_{fc\_x_{time}} \int_{t_0}^{t_0+t} \frac{P_{fc_x}(t)}{P_{fc_{N_x}}(t)} dt \tag{2}$$

Discretizing Equation (2) according to the backward-Euler method, a linear model can be obtained to determine the accumulated degradation considering the instantaneous delivered power, Expression (3).

$$D_{fc_x}(k+1) = P_{fc_x}(k) \cdot \frac{\Delta V_{fc\_x_{time}}}{P_{fc_{N_x}}(k)} \cdot \frac{1\,\text{h}}{3600\,\text{s}} \cdot T_s + D_{fc_x}(k) = P_{fc_x}(k) \cdot D_x(k) + D_{fc_x}(k) \tag{3}$$

where:

$D_x(k)$: Groups all the terms that multiply; $P_{fc_x}(k)$ associated to stack x at sampling time k (V/W).

Based on each stack degradation, it is possible to determine the remained rated power value, $P_{fc_{N_x}}(k+1)$, according to the accumulated stack degradation, D_{fc_x}, and the nominal current, $I_{fc_{N_x}}$, at sampling time k, Expression (4):

$$P_{fc_{N_x}}(k+1) = P_{fc_{N_x}}(k) - D_{fc_x}(k) \cdot I_{fc_{N_x}} \tag{4}$$

3.1.3. Multi-Stack FC System Cost

The operating cost of each stack, C_{fc_x}, in €, will be defined by 2 power variable terms associated with the operation and maintenance (O&M) costs and the depreciation cost [31]. The last term will be defined by the equipment acquisition cost, C_{x_0}, the degradation associated with the operating power,

D_x, and the maximum expected degradation, $D_{fc_{max}}$, Expression (5). Unlike the degradation term, the optimization of the overall multi-stack FC system cost can be ensured by minimizing the economic cost function in each sampling period. For this reason, it was not necessary to take into account the accumulated cost.

$$C_{fc_x}(k+1) = P_{fc_x}(k) \cdot \left(C_{O\&M_{fc_x}} + C_{x_0} \frac{D_x(k)}{D_{fc_{max}}} \right) \cdot \frac{1 \text{ h}}{3600 \text{ s}} \cdot T_s = P_{fc_x}(k) \cdot C_x(k) \tag{5}$$

where:

$C_x(k)$: Groups all the terms that multiply $P_{fc_x}(k)$ associated with stack x at sampling time k (€/W)

Considering the Expression (5), the overall cost of the multi-stack FC system, C_{sys}, can be calculated as the sum of the individual costs, Expression (6).

$$C_{sys}(k+1) = \sum_{x=1}^{n} C_{fc_x}(k) \tag{6}$$

3.1.4. Multi-Stack FC System Hydrogen Consumption

Regarding the molar hydrogen consumption ratio for each stack, $\dot{n}_{H2}$, it can be calculated considering the Faraday Law [7], which defines linearity with respect to operating current, $I_{fc_x}(k)$, as it is expressed in (7).

$$\dot{n}_{H2}(k) = \frac{N_{cell} \cdot I_{fc_x}(k) \cdot T_s}{z \cdot F} \tag{7}$$

Considering the operating stack voltage in each sampling period, $V_{fc_x}(k)$, it is possible to obtain the expression of the hydrogen consumption ratio, in volume, of each stack, H_{2_x}, as a function of the operating power, as expressed in (8). Like the cost term, the optimization of the overall hydrogen consumption can be ensured by minimizing the consumption ratio in each sampling period. For this reason, it is not necessary to take into account the accumulated consumption.

$$H_{2_x}(k+1) = \frac{\dot{n}_{H2} \cdot M_{H2}}{\rho_{H2}} = \frac{P_{fc_x}(k) \cdot N_{cell(x)} \cdot M_{H2}}{z \cdot F \cdot \rho_{H2} \cdot V_{fc_x}(k)} \cdot \frac{1 \text{ h}}{3600 \text{ s}} \cdot T_s = P_{fc_x}(k) \cdot r_x(k) \tag{8}$$

where:

$r_x(k)$: Groups all the terms that multiply $P_{fc_x}(k)$ associated to stack x at sampling time k (Nm³/Wh).

Considering the Expression (8), the overall hydrogen consumption of the multi-stack FC system, $H_{2_{sys}}$, can be calculated as the sum of each individual consumption, Expression (9).

$$H_{2_{sys}}(k+1) = \sum_{x=1}^{n} H_{2_x}(k) \tag{9}$$

If the stack operating voltage cannot be obtained through direct measurement, it can be estimated from its polarization curve and the accumulated stack degradation, Expression (10). Due to the slow dynamics of this type of system, it is possible to use sampling periods of the order of 10s of seconds, without affecting the performance of the system. Based on the above, the use of static models, such as the polarization curve, allows in a simplified way to obtain an acceptable approximation of the fuel cell's behavior.

$$V_{fc_x}(k) = a - b \cdot \log\left(P_{fc_x}(k-1)\right) - c \cdot P_{fc_x}(k-1) - d \cdot e^{(-e \cdot P_{fc_x}(k-1))} - \sum_{j=1}^{j=k} D_{fc_x}(j) \tag{10}$$

where:

a, b, c, d, e: Fuel cell parameters for voltage model.

3.1.5. Multi-Stack FC System Discrete State-Space Model

With the premises considered in Sections 3.1.1–3.1.4, the generalized LPV discrete state-space model for a multi-stack FC system consisting of n stacks for a given sampling time T_s was presented in (11a) and (11b). This can be expressed in the most compact way as (12).

$$
\underbrace{\begin{bmatrix} D_{fc_1}(k+1) \\ \vdots \\ D_{fc_n}(k+1) \\ P_{sys}(k+1) \\ C_{sys}(k+1) \\ H_{2sys}(k+1) \end{bmatrix}}_{\substack{x(k+1) \\ (n+3)\times 1}}
=
\underbrace{\begin{bmatrix} 1 & \cdots & 0 & 0 & 0 & 0 \\ \vdots & \ddots & 0 & 0 & 0 & 0 \\ 0 & \cdots & 1 & 0 & 0 & 0 \\ 0 & \cdots & 0 & 0 & 0 & 0 \\ 0 & \cdots & 0 & 0 & 0 & 0 \\ 0 & \cdots & 0 & 0 & 0 & 0 \end{bmatrix}}_{\substack{A \\ (n+3)\times(n+3)}}
\cdot
\underbrace{\begin{bmatrix} D_{fc_1}(k) \\ \vdots \\ D_{fc_n}(k) \\ P_{sys}(k) \\ C_{sys}(k) \\ H_{2sys}(k) \end{bmatrix}}_{\substack{x(k) \\ (n+3)\times 1}}
+
\underbrace{\begin{bmatrix} D_1(k) & \cdots & 0 \\ 0 & \ddots & 0 \\ 0 & \cdots & D_n(k) \\ 1 & \cdots & 1 \\ C_1(k) & \cdots & C_n(k) \\ r_1(k) & \cdots & r_n(k) \end{bmatrix}}_{\substack{B \\ (n+3)\times n}}
$$

$$
\cdot
\underbrace{\begin{bmatrix} P_{fc_1}(k) \\ \vdots \\ P_{fc_n}(k) \end{bmatrix}}_{\substack{u(k) \\ n\times 1}}
+
\underbrace{\begin{bmatrix} 1 & \cdots & 0 & 0 & 0 & 0 \\ \vdots & \ddots & 0 & 0 & 0 & 0 \\ 0 & \cdots & 1 & 0 & 0 & 0 \\ 0 & \cdots & 0 & 1 & 0 & 0 \\ 0 & \cdots & 0 & 0 & 1 & 0 \\ 0 & \cdots & 0 & 0 & 0 & 1 \end{bmatrix}}_{\substack{E \\ (n+3)\times(n+3)}}
\cdot
\underbrace{\begin{bmatrix} v_{D_{fc_1}}(k) \\ \vdots \\ v_{D_{fcn}}(k) \\ v_{P_{sys}}(k) \\ v_{C_{sys}}(k) \\ v_{H_{2sys}}(k) \end{bmatrix}}_{\substack{v(k) \\ (n+3)\times 1}}
\tag{11a}
$$

$$
\underbrace{\begin{bmatrix} D_{fc_1}(k) \\ \vdots \\ D_{fc_n}(k) \\ P_{sys}(k) \\ C_{sys}(k) \\ H_{2sys}(k) \end{bmatrix}}_{\substack{y(k) \\ (n+3)\times 1}}
=
\underbrace{\begin{bmatrix} 1 & \cdots & 0 & 0 & 0 & 0 \\ \vdots & \ddots & 0 & 0 & 0 & 0 \\ 0 & \cdots & 1 & 0 & 0 & 0 \\ 0 & \cdots & 0 & 1 & 0 & 0 \\ 0 & \cdots & 0 & 0 & 1 & 0 \\ 0 & \cdots & 0 & 0 & 0 & 1 \end{bmatrix}}_{\substack{C \\ (n+3)\times(n+3)}}
\cdot
\underbrace{\begin{bmatrix} D_{fc_1}(k) \\ \vdots \\ D_{fc_n}(k) \\ P_{sys}(k) \\ C_{sys}(k) \\ H_{2sys}(k) \end{bmatrix}}_{\substack{x(k) \\ (n+3)\times 1}}
\tag{11b}
$$

$$
\underbrace{\begin{bmatrix} v_{D_{fc_1}}(k) \\ \vdots \\ v_{D_{fcn}}(k) \\ v_{P_{sys}}(k) \\ v_{C_{sys}}(k) \\ v_{H_{2sys}}(k) \end{bmatrix}}_{\substack{v(k) \\ (n+3)\times 1}}
=
\underbrace{\begin{bmatrix} D_{fc_1}(k-1) \\ \vdots \\ D_{fc_n}(k-1) \\ P_{sys}(k-1) \\ C_{sys}(k-1) \\ H_{2sys}(k-1) \end{bmatrix}}_{\substack{x(k-1) \\ (n+3)\times 1}}
-
\underbrace{\begin{bmatrix} D_{fc_1}real(k-1) \\ \vdots \\ D_{fcn}real(k-1) \\ P_{sys}real(k-1) \\ C_{sys}real(k-1) \\ H_{2sys}real(k-1) \end{bmatrix}}_{\substack{x_{real}(k-1) \\ (n+3)\times 1}}
$$

Each row in the state Equations (11a) and (11b) can be obtained as follows: $D_{fc_1}(k+1)$ to $D_{fc_n}(k+1)$ from Equation (2). Regarding the power generated by the multi-stack FC system, $P_{sys}(k)$, row $n+1$, it can be obtained from Expression (1). The overall cost, $C_{sys}(k)$, row $n+2$, can be

defined from each individual cost and its sum, Equations (5) and (6), respectively. Finally, hydrogen consumption, $H_{2_{sys}}(k)$, row $n + 3$, comes from (8) and (9).

Regarding $v_{D_{fc_1}}(k)$ to $v_{H_{2_{sys}}}(k)$, represent model disturbances, which are approximated as the error between the value estimated by the model and the real value measured directly on the plant in the previous sample time $k - 1$.

$$x(k+1) = Ax(k) + Bu(k) + Ev(k) y(k) = Cx(k) \tag{12}$$

where:

$x(k)$: State vector $\left[D_{fc_1}(k)\, D_{fc_2}(k) \ldots D_{fc_n}(k)\, P_{sys}(k)\, C_{sys}(k)\, H_{2_{sys}}(k)\right]^T$

$u(k)$: Input vector $\left[P_{fc_1}(k)\, P_{fc_2}(k) \ldots P_{fc_n}(k)\right]^T$

$v(k)$: Model disturbances vector $\left[v_{D_{fc_1}}(k)\, v_{D_{fc_2}}(k) \ldots v_{D_{fcn}}(k)\, v_{P_{sys}}(k)\, v_{C_{sys}}(k)\, v_{H_{2_{sys}}}(k)\right]^T$

$y(k)$: Output vector $\left[D_{fc_1}(k)\, D_{fc_2}(k) \ldots D_{fc_n}(k)\, P_{sys}(k)\, C_{sys}(k)\, H_{2_{sys}}(k)\right]^T$

As can see in Expression (11a), (11b) and (12), the model proposed allows the inclusion of uncertainties in the degradation parameter in the form of perturbations in the output vector. This disturbance vector was estimated based on the difference between the real value obtained from a stack voltage and the value obtained by the model in the previous instant. Thanks to the inclusion of this parameter and the use of predictive control techniques, an intrinsic feedforward action was integrated to estimate the error committed in the model and the correction in the control law.

3.2. MPC Controller

This section describes the formulation of a predictive controller for optimal power generation of a multi-stack FC system, considering constraints, and technical and economic parameters. In this case, a linear constrained MPC controller has been used, in which the solution of the optimization problem is done by Quadratic programming (QP).

The main objective of the controller was always to guarantee the operating power defined by the EMS that governs the microgrid. The second objective was to operate the FC system under optimal considerations, increasing its lifespan, and reducing the operating losses and cost. For this purpose, the controller calculates the optimal power distribution of the multi-stack FC system, considering the accumulated equipment degradation, current hydrogen consumption, and operating cost.

The proposed control scheme is shown in Figure 3, where n manipulated variables have been assigned to the controller, corresponding to the output power of each of the stacks in the modular system, $P_{fc_x}(k)$.

The multi-stack FC system outputs have been defined as the instantaneous degradation of each stack, $D_{fc_x}(k)$, as well as the total generated power, $P_{sys}(k)$, total hydrogen consumed, $H_{2_{sys}}(k)$, and operating and maintenance cost of the complete multi-stack FC system, $C_{sys}(k)$.

Finally, the controller receives the power setpoint of the multi-stack FC system, $P_{REF}(k)$, calculated by the overall microgrid EMS in each sampling time k. This strategy allows the power reference of the modular system to be included in the control scheme.
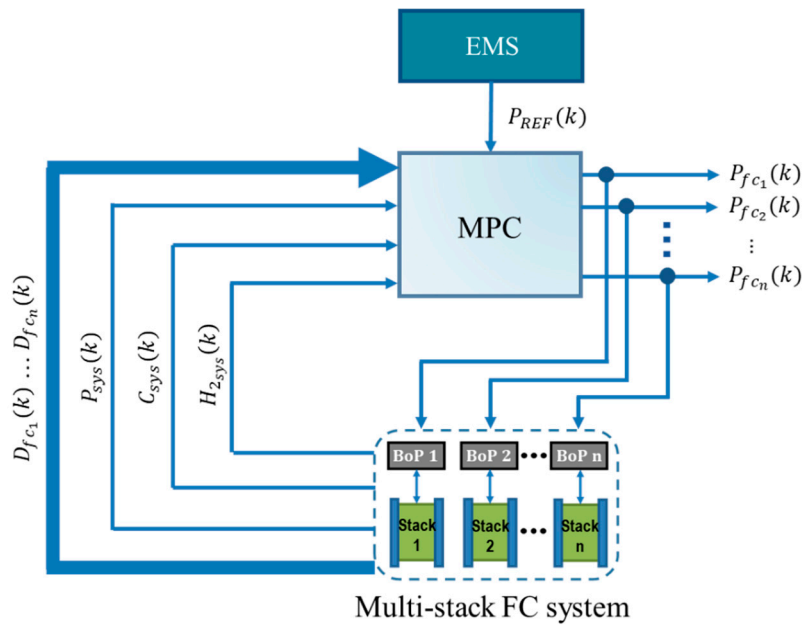
Figure 3. MPC controller architecture for the proposed multi-stack FC system.

3.2.1. Objective Function

According to the general formulation of the MPC controller, the objective function to be solved at each sampling time k is given by Expression (13).

$$J = \sum_{j=1}^{N_p} \alpha(j)\left[\hat{y}(k+j|k) - r(k+j)\right]^2 + \sum_{j=1}^{N_u} \lambda(j)\left[\Delta u(k+j-1)\right]^2 \tag{13}$$

where:

N_p: Prediction horizon.

N_u: Control horizon.

$\alpha(j)$: Weighting factor of output tracking error.

$\hat{y}(k+j|k)$: Output prediction at sampling time $k+j$ based on measurements known at sampling time k.

$r(k+j)$: Output reference at sampling time $k+j$.

$\lambda(j)$: Weighting factor that penalizes, from sampling time k, changes in the control action.

$\Delta u(k+j-1)$: control action at sampling time $k+j-1$.

In this controller proposal, it is posed a tracking problem, in which the main objective of the control system is established, the tracking of the reference power, $P_{REF}(k)$.

Similarly, the cost function presents an economic optimization problem, in which individual fuel cell degradations are considered, as well as the system cost and hydrogen consumption. This raises a multi-objective optimization problem, which allows a more conservative use of the system from a technical and economic point of view according to the weighting factors, $\alpha(k)$.

Finally, a term associated with the weighting of the change in operating power is included, $\Delta P_{fc_x}(k)$, thus that operating conditions related to system dynamics can be established, with the appropriate tuning of the weighting factors, $\lambda(k)$.

Based on the above, and particularizing (13) for the LPV system model, (11a) and (11b), the designed cost function is presented in (14):

$$J_k = \sum_{x=1}^{n} \alpha_x \left(D_{fc_x}(k)\right)^2 + \alpha_{n+1}\left(P_{sys}(k) - P_{REF}(k)\right)^2 + \alpha_{n+2}\left(C_{sys}(k)\right)^2 + \alpha_{n+3}\left(H_{2_{sys}}(k)\right)^2 + \sum_{x=1}^{n} \lambda_x \Delta P_{fc_x}^2(k) \tag{14}$$

where:

$P_{REF}(k)$: Multi-stack FC system reference power at sampling time k (W).

$\Delta P_{fc_x}(k)$: Variation of power delivered by each stack at sampling time k.

3.2.2. Constraitns

Model predictive control is an optimization control algorithm that allows managing constrained optimization problems. In general, the optimization problem allows considering constraints of the output vector and magnitude and dynamics of the control vector, Expression (15). These constraints are normally restrictions imposed by the operating conditions of the real plant.

$$
\begin{aligned}
y_{min} \leq y \leq y_{max} \\
u_{min} \leq u \leq u_{max} \\
\Delta u_{min} \leq \Delta u \leq \Delta u_{max}
\end{aligned}
\tag{15}
$$

Restrictions on system output variables, $D_{fc_x}(k)$, $P_{sys}(k)$, $C_{sys}(k)$ and $H_{2_{sys}}(k)$ are imposed by the real limits, i.e., always degradation, cost, and hydrogen consumption must be positive values, and the multi-stack FC system output power should obviously be lower than the sum of individual stacks nominal power in the sampling time k.

Similarly, the maximum operating power of each stack, $P_{fc_x}(k)$, will be given by the nominal power value considering the accumulated degradation, $P_{fc_{N_x}}(k)$.

Finally, with the aim of making conservative use of the stacks, the constraints regarding the power slew rate for the manipulated variables, $\Delta P_{fc_x}(k)$, are established.

Based on the above, and particularizing (15) for the LPV system model, Expression (11a) and (11b), the system constraints are presented in (16):

$$
\begin{aligned}
D_{fc_x}(k) \geq 0 \\
0 \leq P_{sys}(k) \leq \sum_{x=1}^{n} P_{fc_{N_x}}(k) \\
C_{sys}(k) \geq 0 \\
H_{2_{sys}}(k) \geq 0 \\
0 \leq P_{fc_x}(k) \leq P_{fc_{N_x}}(k) \\
-1000\ W \leq \Delta P_{fc_x}(k) \leq 1000\ W
\end{aligned}
\tag{16}
$$

3.2.3. Tuning

The main objective of the MPC controller was to ensure that the power reference demanded by the EMS was met, fulfilling the premises of minimum degradation of the stacks and minimum costs and losses of the multi-stack FC system. Considering the objective function, Expression (14), the tuning of the weighting factors (α_x, α_{n+1}, α_{n+2}, α_{n+3}, and λ_x, being, $x = 1 \ldots n$,) will allow the problem to be tailored to the fundamental objective determined by the design criteria.

Assuming there is a great amount of controller parameters, the analytical tuning process can be very complex, and that is why it was proposed to face it in a heuristic way. To that end, a set of cause-effect relationships that can help the tuning process was defined.

In the first instance, to increase the lifespan of the multi-stack FC system, the tuning analysis focused on the power distribution according to the accumulated degradation of each stack. In this way, the stack that develops higher degradation will have a greater associated weighting factor inside the objective function (penalty), Expression (14), which will limit its operating power to the detriment of those stacks with less accumulated degradation. For this purpose, α_x must have a high value and it is estimated considering the accumulated degradation with respect to the maximum one.

In response to the main objective of the controller, to assure the reference power at all times, the weighting factor associated with the output power tracking error, α_{n+1}, must have a high value

(it acts as a strong constraint), in such a way that any difference between $P_{sys}(k)$ and $P_{REF}(k)$ should be penalized.

The weighting factor α_{n+2} determines the weight of the economic objective in the optimization problem. Because the cost term is closely related to the multi-stack FC system degradation, the increase in the lifetime of the system will be translated in a parallel way into a cost reduction. Considering the fundamental objectives of the controller, the reduced value of the weighting parameter will be used, thus that the weight of this term was reduced, in favor of the technical optimization.

Weighting factor α_{n+3} was related to the hydrogen consumption of the multi-stack FC system, thus that the use of a high value of the weighting factor will result in more balanced power distribution between stacks thus that the hydrogen resource is used more efficiently. Increasing system performance was a fundamental objective in the design criteria of the controller, and, therefore, a relatively high value of the associated weighting parameter is used.

Finally, the term associated with the control effort, λ_x, can be used to reduce power variations and, therefore, avoid abrupt changes in the power setpoints of the stacks. As the sampling period was relatively large (in fact, in practice, it was set at 1 minute), and considering the restrictions on power variation, reduced values of this parameter can be used, thus that the penalty for variation of the operating point was not a critical parameter.

Based on the design criteria and after some trial and error cycles, the controller parameters were heuristically tuned (please, see Table 3).

Table 3. Controller parameters.

Parameter	Value
T_s	60 s
N_p N_u: Control horizon.	5
N_u N_u: Control horizon.	5
α_x	10 (*)
α_{n+1}	250
α_{n+2}	0.005
α_{n+3}	2
λ_x	2×10^{-8}

(*) Initially, the same degradation is considered for all the stacks. As each stack is put into operation, the respective accumulated degradation varies.

4. Results

The MPC control strategy presented in this work has been carried out under Matlab® environment, simulating an interval of 1125 days. This interval has been determined considering the time when the first stack of the multi-stack FC system reaches the end of its lifespan in the most favorable case. Given that the stack degradation has been quantified in terms of the voltage drop, the criterion taken to establish that a stack has reached the end of its useful life has been that this voltage has dropped 100 mV/cell. In this case, as each stack was made up of 80 cells, the voltage drop at the stack output will be 8 V with respect to its nominal operating conditions.

To analyze the effectiveness of the proposed MPC controller in terms of extending the stack lifespan, minimizing hydrogen consumption, and reducing costs, according to the multi-objective, the multi-stack configuration was compared with two other FC systems. The first one was a single-stack FC system of 7.5 kW (the nominal power of the single-stack FC system coincides with the sum of the three stacks-based FC system proposed by authors). The model was similar to that developed in Section 3.1 but considering a single stack that must always supply the demanded power. The second comparison was made with a multi-stack FC system (also three stacks) that works under an equidistribution strategy that shares the required power between the stacks uniformly. Table 4 shows the degradation rates

associated with stacks in all the considered cases, according to the number of cells, and the average, maximum, and minimum values determined by the tolerances given by the manufacturer [26]. As has been commented in Section 3.1.2, the degradation rate was an experimentally calculated parameter. For this purpose, a cell voltage monitoring system (CVM) was used [27]. This CVM monitors the cells' voltage with the aim to evaluate the total degradation accumulated by the stack (stack degradation is the sum of cell degradation). For the single-stack FC system, the considered degradation rate corresponded to the average degradation of the multi-stack FC system.

Table 4. Fuel cell degradation rates.

Stack Voltage Drop Case 1 (Single Stack)	Value	Stack Voltage Drop Case 2: Multi-Stack with Equi-Distribution Case 3: Multi-Stack with MPC	Value
		$\Delta V_{fc\_1_{time}}$	960×10^{-6} V/h (12×10^{-6} V/h·cell)
$\Delta V_{fc_{time}}$	960×10^{-6} V/h (12×10^{-6} V/h·cell)	$\Delta V_{fc\_2_{time}}$	1200×10^{-6} V/h (15×10^{-6} V/h·cell)
		$\Delta V_{fc\_3_{time}}$	720×10^{-6} V/h (9×10^{-6} V/h·cell)

The sampling time chosen was 1 minute since it was short enough considering that the objective of the paper was to check the performance of the strategy along the whole lifetime of the FC system (1125 days).

Figure 4a shows the power profile that the EMS of the microgrid demands from the FC system (please see Figure 3). This power profile has been chosen because it allows achieving different power steps that force the multi-stack FC system works in different operating regimes and, therefore, allow to validate the MPC controller performance. The same profile was repeated for the 1125 days with the aim to compare three fuel cell systems along all is lifespan. To carry out this comparison, a common load profile repeated during the whole period was needed. Figure 4b shows the reference power tracking performance for the three cases. The reference power is always met by the FC system in the three cases.
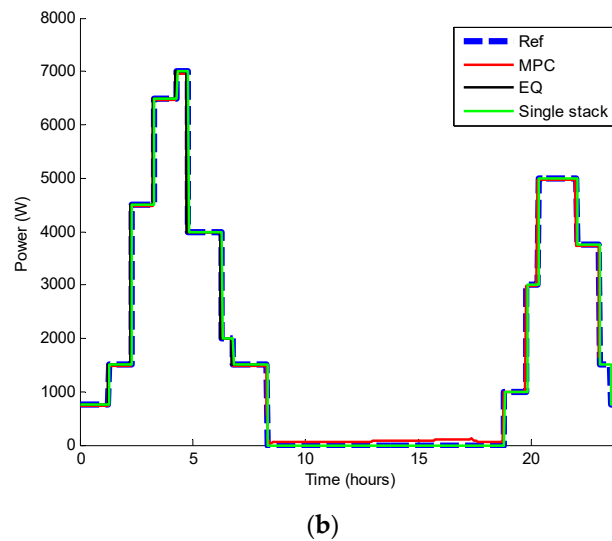

(a)

Figure 4. *Cont.*

(b)
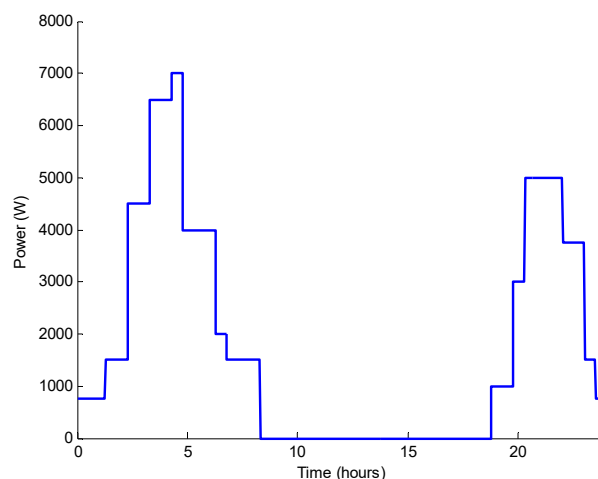
Figure 4. (**a**). Power profile required by the energy management system (EMS) of the microgrid. (**b**). Reference power tracking performance for single stack, equal power distribution, and MPC cases with respect reference power profile.

The stacks degradation is represented in Figure 5. $DFC_{single\text{-}stack}$ corresponds to the degradation in the single-stack FC system (case 1), $DFC1_{EQ}$, $DFC2_{EQ}$, and $DFC3_{EQ}$ represent the degradation of the stacks 1, 2, and 3, respectively, in case 2 (multi-stack FC system with equal power distribution), and $DFC1_{MPC}$, $DFC2_{MPC}$, and $DFC3_{MPC}$ show the degradation of the stacks 1, 2, and 3, respectively, in case 3 (multi-stack FC system with proposed MPC control algorithm). As was explained in Section 3, degradation was associated with the maximum power that each stack can provide at every moment. The proposed control algorithm gave greater relevance to the current degradation to carry out the power distribution between the stacks of the FC system.
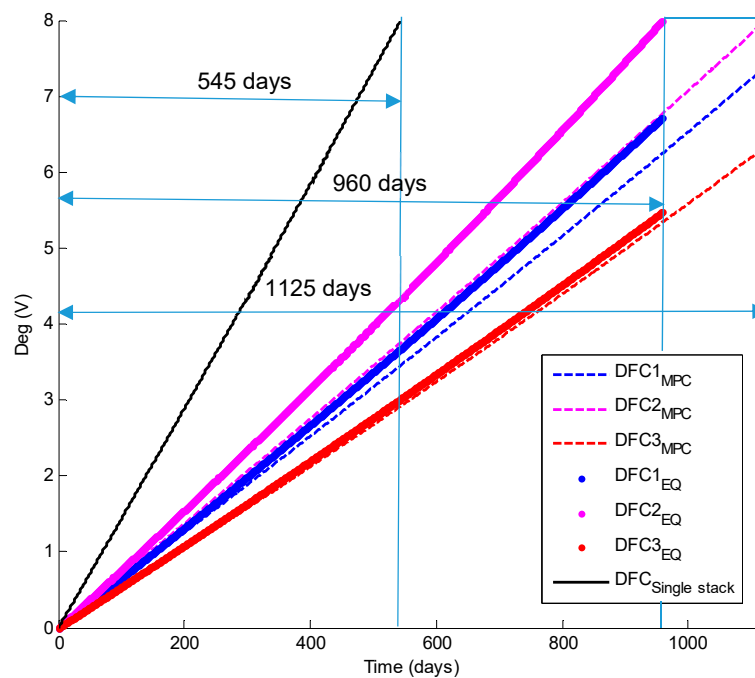

Figure 5. Comparative of stacks degradation in the three cases (single-stack FC system, multi-stack FC system with equal power distribution, and multi-stack FC system with MPC controller). Single-stack lifespan: Day 545. Multi-stack FC system with equal power distribution lifespan: day 960. Multi-stack FC system with MPC control algorithm lifespan: Day 1125.

Another output variable of the developed state-space model was hydrogen consumption, drawn in Figure 6a. Detailed plots at the end of the lifespan of the single-stack FC system were highlighted in Figure 6b, and at the end of the lifespan of the multi-stack FC system in Figure 6c. As before, it has been represented the hydrogen consumption in the three cases: Single-stack FC system, multi-stack FC system with equal power distribution, and multi-stack FC system with the proposed MPC control algorithm.
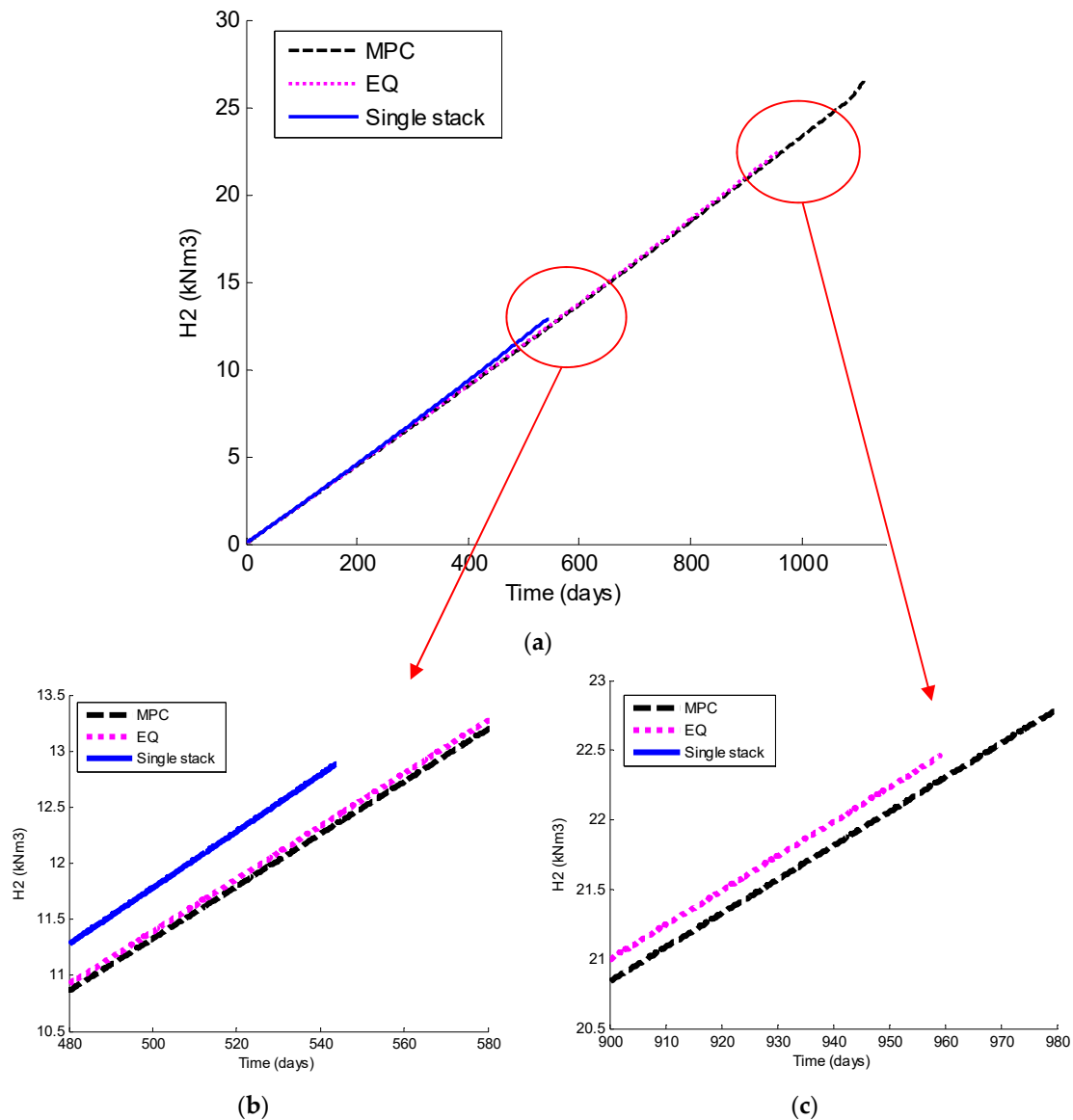

Figure 6. (**a**) Hydrogen consumption of the FC system in the three cases (single-stack FC system, multi-stack FC system with equal power distribution, and multi-stack FC system with MPC controller). (**b**) Detail to highlight the multi-stack FC system with MPC regarding the single stack system. (**c**) Detail to highlight the multi-stack FC system with MPC regarding the multi-stack FC system with equal power distribution (1 kNm^3 = 10^3 Nm^3).

Finally, Figure 7 shows the costs of each analyzed FC system (O&M costs and the depreciation cost) throughout their respective lifespan.

To summarize the obtained results, Table 5 offers a comparison between the three considered scenarios (single-stack FC system, multi-stack FC system with equal power distribution, and multi-stack FC system with the proposed MPC control algorithm). The comparison has been done in terms of stack degradation, hydrogen consumption, and cost. Note that the data have been taken from the day when

the single-stack FC system has arrived at the end of its lifespan, day 545 (Figure 5 and Table 5a,b shows the values of day 960, when the first stack of the multi-stack FC system under equal power operation reached its maximum degradation value. Finally, Table 5c shows the values obtained at the end of the lifespan of the multi-stack FC system with the MPC controller developed in this work. This situation occurs on day 1125 of operation.
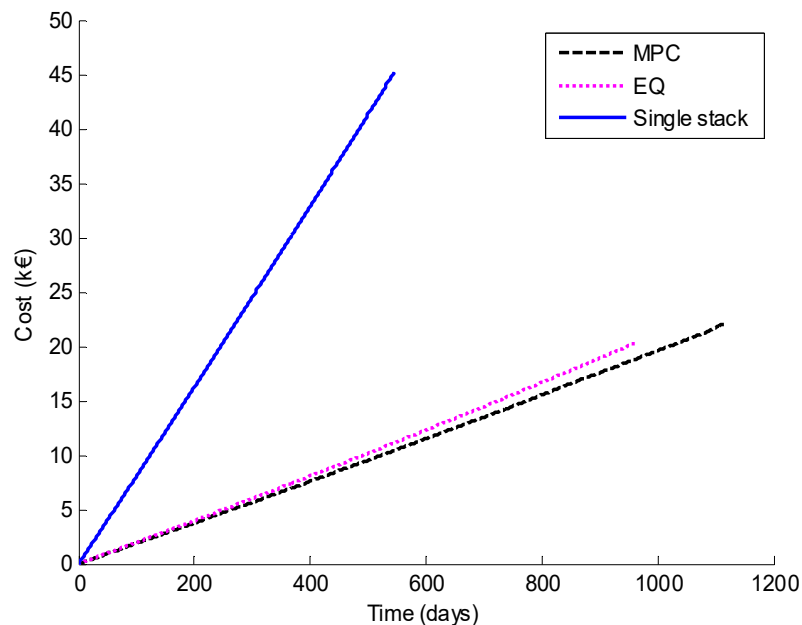

Figure 7. Operating costs of the FC system in the three cases (single-stack FC system, multi-stack FC system with equal power distribution, and multi-stack FC system with MPC controller) (1 k€ = 10^3 €).

Table 5. Simulation results.

Cases Analyzed	Degradation (Volts)				H$_2$ (kNm^3)	Cost (K€)
	Single Stack	Stack 1	Stack 2	Stack 3		
Single-stack	8.007				12.886	45.063
Multi-stack Equ-Distribution		3.682	4.352	3.022	12.426	11.078
Multi-stack MPC		3.452	3.754	2.917	12.360	10.147

(a)　Day 545 (single-stack FC system at the end of its lifespan)

Cases Analyzed	Degradation (Volts)				H$_2$ (kNm^3)	Cost (K€)
	Single Stack	Stack 1	Stack 2	Stack 3		
Single stack	-				-	-
Multi-stack Equ-Distribution		6.722	8.006	5.479	22.458	20.247
Multi-stack MPC		6.240	6.762	5.333	22.254	18.375

(b)　Day 960 (multi-stack FC system with equal distribution at the end of its lifespan)

Cases Analyzed	Degradation (Volts)				H2 (kNm3)	Cost (K€)
	Single Stack	Stack 1	Stack 2	Stack 3		
Single stack	-				-	-
Multi-stack Equ-Distribution		-	-	-	-	-
Multi-stack MPC		7.392	8.004	6.339	26.298	21.779

(c)　Day 1125 (multi-stack FC system with proposed MPC at the end of its lifespan)

Background color is necessary to indicate that these positions are not possible.

Graphs depicted in Figure 8 illustrates the evolution of the delivered power (plots on the left) and the voltage supplied (plots on the right) by the three stacks of the multi-stack FC operating with the MPC controller, at different times throughout the simulation period.
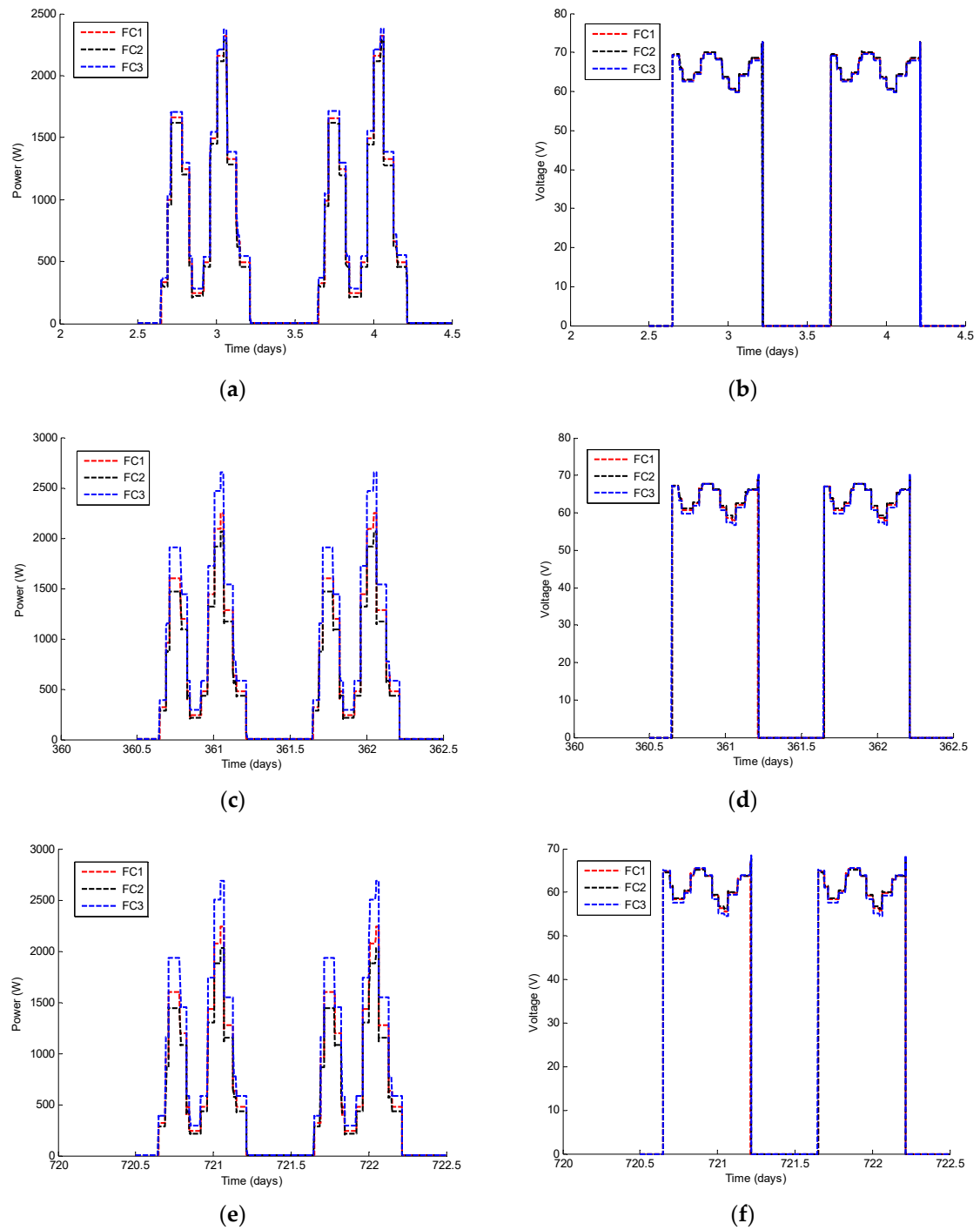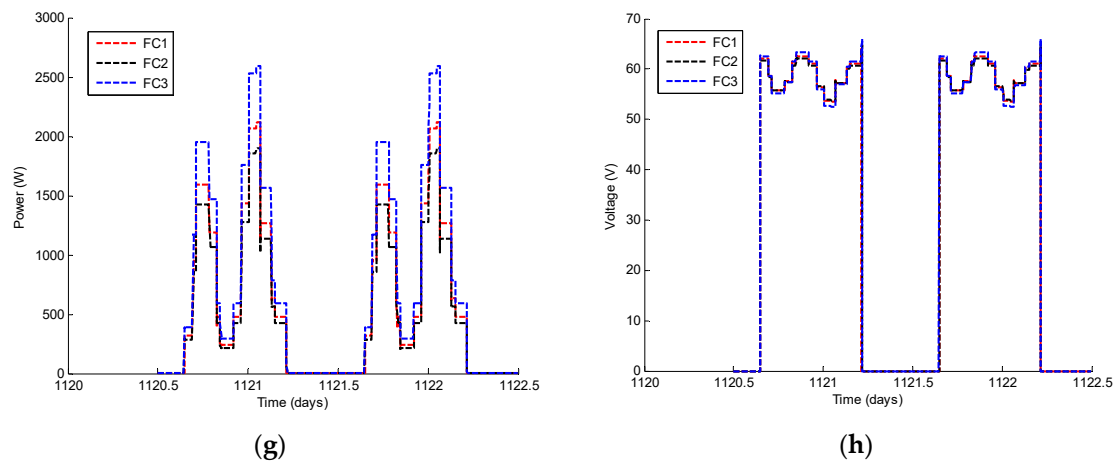

Figure 8. *Cont.*

Figure 8. Delivered power and voltage of the stacks 1, 2, and 3 of the multi-stack FC system operating with MPC controller at different times. (**a**,**b**) Days 3 and 4. (**c**,**d**) Days 361 and 362. (**e**,**f**) Days 721 and 722. (**g**,**h**) Days 1121 and 1122.

5. Discussion

Based on obtained results, as can be appreciated in Figure 5, the degradation of the FC system is considerably higher in the case of using a single stack to provide the power demanded by the EMS. The lifespan in the case of a single stack decreases something more than 50% compared to the case of using the proposed MPC controller to manage the multi-stack FC system. Furthermore, in the case of using a multi-stack FC system, the lifespan of the whole system also increases when the proposed MPC controller is applied to carry out the power distribution. The degradation by using the proposed MPC controller is lower because the operating power is calculated to minimize the degradation of the system, and, therefore, makes a power distribution between stacks based on the degradation level of each one.

Additionally, the controller parameters have been selected before carrying out the simulations (Table 3), α_x has been set the same for all the stacks, thus, $\alpha_1 = \alpha_2 = \alpha_3 = 10$ in the simulations, which would logically correspond to a set of brand new stacks. Therefore, there is no preference for deteriorating (or preserving) some stacks more than others. Thus, depending on the degradation dynamic of each stack, this will be its lifespan. In that way, as stack 2 has a higher deterioration dynamic value, this is the first that finishes its lifespan. However, if the stacks are not brand new, with different initial conditions (with respect to their degradation degree), it is possible to tune (even adaptively) each α_x depending on this. For that, it is compulsory to know at any time the degradation degree of each stack. This has been resolved by authors [27,29,30]. Based on these developments, it is possible that even from brand new stacks with the same α_x at the beginning of their operation, knowing the degradation degree in real-time for each stack, it is feasible to adapt it looking for a uniform degradation degree for all stacks, pursuing that all reach the same lifespan. That is, achieving that all the characteristics (DFC1$_{MPC}$, DFC2$_{MPC}$ y DFC3$_{MPC}$) coincide in Figure 5.

Regarding hydrogen consumption, as can be seen in Figure 6a, at the beginning of the lifespan of the stacks, hydrogen consumption is similar in the three cases. However, as the stacks are degraded, the voltage decreases. Hence, to provide the same power, a higher current is required, and, according to Faraday's Law, hydrogen consumption increases; therefore, the greater the degradation, the greater the hydrogen consumption. Therefore, taking into account that FC electrical efficiency is directly related with hydrogen consumption, systems operating at the same power, Figure 4b, but with different hydrogen consumption, Figure 6b (single-stack FC system consumes more hydrogen than multi-stack with equal power distribution, and FC system with equal power distribution consumes more hydrogen than multi-stack with MPC) reveals that MPC-based control strategy improves the

FC system performance. The percentage of efficiency improvement coincides with the percentage of hydrogen consumption reduction.

This situation is even worse in the case of a single stack FC system, where hydrogen consumption increases notably. Likewise, it can be verified that the hydrogen consumption of the multi-stack system applying the MPC control strategy developed in this work is slightly lower than in the case of equal power distribution operation, as can be appreciated in Figure 6c. From the analysis of these figures, it can be established that hydrogen consumption worsens more as the degradation of the stacks increases.

The degradation optimization implies a reduction in depreciation costs, as the lifespan is extended. As shown in Figure 7, the cost of the single-stack FC system is very high compared to the multi-stack one. Really, the final cost, if the availability of power needs to be satisfied over time, is considerably higher, because it would be necessary to add the replacement cost to equalize the lifespan of the multi-stack FC system.

On the other hand, a decrease in costs is also observed in a multi-stack FC system if the proposed MPC algorithm is used instead of the uniform power distribution.

The analysis of the data presented in Table 5 emphasizes what was previously commented on. There is a noticeable difference between using a single-stack and using a multi-stack system in terms of lifespan and costs (both in terms of O&M and depreciation cost). In the case of the multi-stack FC system with equal power distribution, while the single-stack is fully degraded at day 545, stack 1 is degraded at 45.9%, stack 2 at 54.3%, and stack 3 at 37.7%. The hydrogen consumption is reduced by 3.6% (consequently, the FC system efficiency is improved in the same percentage), and a cost-saving of 75.4%. This difference is even more pronounced in the case of the multi-stack FC system with MPC-based control; stack 1 is degraded at 43.1% for stack 1, stack 2 at 54.3%, and stack 3 at 36.4%. The hydrogen consumption is reduced by 4% (same percentage for the efficiency improvement), and a cost-saving of 77.4%.

Taking into account the time when the FC system arrives at the end of its lifespan, an increase of 76.4% is observed in the stacks lifespan of the multi-stack FC system with equal power distribution compared to the single-stack FC system. This improvement reaches 106.8% in the case of the multi-stack FC system based on the proposed MPC controller compared to the single-stack FC system.

In each sampling period, the power delivered by each stack (Figure 8) is corrected (this is due to the application to the multi-stack system), since it depends on the degradation suffered by the corresponding stack. Since the stack voltage is progressively decreasing due to degradation, stacks would need to supply higher current to provide the same power, increasing the hydrogen consumption. The multi-stack FC system is connected to the microgrid by means DC/DC converters (Figure 1), therefore, despite the fact that the stacks output voltages vary, the power conditioning stages guarantee the DC bus voltage.

As results show, starting from three brand new stacks, the degradation dynamic of each one is different (in fact, the own manufacturer informs of a tolerance, within it which can be any of the stacks), thus, over time, the degree of degradation of each stack is different and, therefore, the voltage level and obviously the power delivered of each one is also different.

Focused on the multi-stack FC system, analyzing the time intervals shown in Figure 8 (please follow the sequence (a) to (h) with the reading), it can be observed that the power delivered by each stack to satisfy the total power requirement is very similar at the beginning of their lifespan because the three stacks present similar initial degradation. However, as the days go by, stack 3 is less damaged than stack 1, and stack 1 is less damaged than stack 2, thus the MPC controller establishes that the power supplied by each stack must be different (lower degradation, the higher capability to supply power). Therefore, the MPC controller guarantees the degradation of all the stacks is homogenized, preserving the lifespan of the most degraded one and, hence, prolonging the lifespan of the multi-stack system.

In summary, the MPC-based proposal presented in this work achieves an optimization, both technical and economic, of the whole FC system in the short and the long term.

6. Conclusions

In this paper, a multi-objective model predictive control (MPC) has been developed for the power management of a multi-stack FC system integrated into a renewable sources-based microgrid. The MPC controller has solved the problem related to the power dispatch to the microgrid while including criteria to reduce the multi-stack FC degradation, O&M costs, as well as hydrogen consumption.

For this purpose, a generalized state-space model of the multi-stack FC system has been developed that allows predicting the future output of the FC system by means of the MPC controller. The model includes both technical and economic variables like stack degradation, hydrogen consumption, and O&M cost, and depreciation cost. In addition, the proposal presents the advantage that all the state vector is measurable, thus it is fully available to carry out, practically and easily, control strategies based on the state vector feedback.

The developed model is defined as an LPV model, which allows defining the non-linear behavior of the multi-stack FC system as a linearized model in each sampling period. Obtained results demonstrate that the multi-stack FC systems working under the developed MPC controller meet with the microgrid power demand over time; but also, at the same time, the stacks degradation and consequently, hydrogen consumption and the total cost of operating the FC system, are reduced regarding other previous solutions found in the scientific literature. In fact, as both the number of stacks in the FC and jumps in power demand of the microgrid increase, the supremacy of the developed solution also increases.

The novelty of this paper lies in the proposal of a generalized MPC controller for a multi-stack FC that can be used independently of the number of stacks that make it up. The controller takes advantage of the characteristics of the multi-stack FC concept, distributing operation across all the stacks regarding their capacity to produce energy and optimizing the overall microgrid performance.

List of Acronyms

CVM   Cell voltage monitoring system
EMS   Energy management system.
ESS   Energy storage system.
FC   Fuel cell.
LPV   Linear parameter variant.
MILP   Mixed integer linear programming.
PEM   Polymer electrolyte membrane.
QP   Quadratic programming.
RES   Renewable energy sources.

Notation and Symbols

$\alpha(j)$ Weighting factor of output tracking error.
$C_{fc_x}(k)$ Total operating cost of the stack x at sampling time k (€).
$C_{O\&M_{fc_x}}$ Operation and maintenance cost of the stack x (0.00004 €/Wh).
$C_{sys}(k)$ Multi-stack FC system cost at sampling time k (€).
C_{x_0} Acquisition cost of the stack x (8000 €).
$\Delta P_{fc_x}(k)$ Variation of power delivered by each stack at sampling time k.

$\Delta u(k+j-1)$	Control action at sampling time $k+j-1$.
$\Delta V_{fc\_x_{time}}$	Voltage drop of the stack x considering the operating hours and cycles (V/h).
$\Delta V_{fc_{Max}}$	Maximum expected fuel cell voltage drop considering the operating hours and cycles (V).
$D_{fc_{max}}$	Maximum expected degradation (0.1 V).
$D_{fc_x}(k)$	Degradation of the stack x at sampling time k (V).
D_x	Degradation associated with the operating power.
F	Faraday constant (26.81 Ah/eq).
$H_{2_{sys}}(k)$	Hydrogen consumption of the muti-stack fuel cell system at sampling time k (Nm^3).
$H_{2_x}(k)$	Hydrogen consumption of the stack x at sampling time k (Nm^3).
$I_{fc_x}(k)$	Operating current of the stack x at sampling time k (A).
$I_{fc_{N_x}}$	Nominal current of the stack x (A).
$\lambda(j)$	Weighting factor that penalizes, from sampling time k, changes in the control action.
M_{H2}	Molecular hydrogen molar mass (2.02 g/mol).
N_{cell}	Number of cells in the stack.
N_p	Prediction horizon (5).
N_u	Control horizon (5).
$\dot{n}_{H2}(k)$	Molar hydrogen consumption ratio of the stack x at sampling time k (mol/h).
$P_{fc_x}(k)$	Operating power of the stack x at sampling time k (W).
$P_{fc_{N_x}}(k)$	Nominal power of the stack x at sampling time k (W).
$P_{REF}(k)$	Multi-stack FC system reference power at sampling time k (W).
$P_{sys}(k)$	Output power of the multi-stack FC system at sampling time k (W).
$r(k+j)$	Output reference at sampling time $k+j$.
$r_x(k)$	Hydrogen consumption ratio of the stack x at sampling time k (Nm^3/h).
ρ_{H2}	Molecular hydrogen gas density (0.0899 Kg/Nm^3).
T_s	Sampling period (s).
$V_x(k)$	Operating voltage of the stack "x" at sampling time k (V).
$\hat{y}(k+j|k)$	Output prediction at sampling time $k+j$ based on measurements known at sampling time k.
z	Number of electrons involved in the reduction-oxidation reaction ($z=2$).

References

1. Zhong, S.; Huang, C. Climate change and human health: Risks and responses. *Chin. Sci. Bull.* **2019**, *64*, 2002–2010. [CrossRef]
2. Helm, D. The European framework for energy and climate policies. *Energy Policy* **2014**, *64*, 29–35. [CrossRef]
3. Gielen, D.; Saygin, D.; Wagner, N. *Renewable Energy Prospects: United States of America*; International Renewable Energy Agency (IRENA): Abu Dhabi, UAE, 2015.
4. Qi, Y.; Ma, L.; Zhang, H.; Li, H. Translating a Global Issue into Local Priority. *J. Environ. Dev.* **2008**, *17*, 379–400. [CrossRef]
5. Ton, D.T.; Smith, M.A. The U.S. Department of Energy's Microgrid Initiative. *Electr. J.* **2012**, *25*, 84–94. [CrossRef]
6. Martin, J.S.; Zamora, I.; Martín, J.J.S.; Aperribay, V.; Eguia, P. Hybrid fuel cells technologies for electrical microgrids. *Electr. Power Syst. Res.* **2010**, *80*, 993–1005. [CrossRef]
7. Ferrario, A.M.; Vivas, F.J.; Manzano, F.S.; Andújar, J.M.; Bocci, E.; Martirano, L. Hydrogen vs. Battery in the Long-term Operation. A Comparative between Energy Management Strategies for Hybrid Renewable Microgrids. *Electronics* **2020**, *9*, 698. [CrossRef]
8. Heras, A.D.L.; Vivas, F.; Manzano, F.S.; Andújar, J.M. From the cell to the stack. A chronological walk through the techniques to manufacture the PEFCs core. *Renew. Sustain. Energy Rev.* **2018**, *96*, 29–45. [CrossRef]
9. Vivas, F.; Heras, A.D.L.; Manzano, F.S.; Andújar, J.M. A review of energy management strategies for renewable hybrid energy systems with hydrogen backup. *Renew. Sustain. Energy Rev.* **2018**, *82*, 126–155. [CrossRef]
10. Yoldaş, Y.; Önen, A.; Muyeen, S.M.; Vasilakos, A.V.; Alan, I. Enhancing smart grid with microgrids: Challenges and opportunities. *Renew. Sustain. Energy Rev.* **2017**, *72*, 205–214. [CrossRef]

11. Kamel, A.A.; Rezk, H.; Shehata, N.; Thomas, J. Energy Management of a DC Microgrid Composed of Photovoltaic/Fuel Cell/Battery/Supercapacitor Systems. *Batteries* **2019**, *5*, 63. [CrossRef]

12. Anastasiadis, A.G.; Konstantinopoulos, S.A.; Kondylis, G.; Vokas, G.A.; Papageorgas, P. Effect of fuel cell units in economic and environmental dispatch of a Microgrid with penetration of photovoltaic and micro turbine units. *Int. J. Hydrogen Energy* **2017**, *42*, 3479–3486. [CrossRef]

13. Li, Q.; Chen, W.; Liu, Z.; Li, M.; Ma, L. Development of energy management system based on a power sharing strategy for a fuel cell-battery-supercapacitor hybrid tramway. *J. Power Sources* **2015**, *279*, 267–280. [CrossRef]

14. Marx, N.; Boulon, L.; Gustin, F.; Hissel, D.; Agbossou, K. A review of multi-stack and modular fuel cell systems: Interests, application areas and on-going research activities. *Int. J. Hydrogen Energy* **2014**, *39*, 12101–12111. [CrossRef]

15. Marx, N.; Hissel, D.; Gustin, F.; Boulon, L.; Agbossou, K. On the sizing and energy management of an hybrid multistack fuel cell—Battery system for automotive applications. *Int. J. Hydrogen Energy* **2017**, *42*, 1518–1526. [CrossRef]

16. Palma, L.; Enjeti, P. A Modular Fuel Cell, Modular DC–DC Converter Concept for High Performance and Enhanced Reliability. *IEEE Trans. Power Electron.* **2009**, *24*, 1437–1443. [CrossRef]

17. Garcia, J.E.; Herrera, D.F.; Boulon, L.; Sicard, P.; Hernandez, A. Power Sharing for Efficiency Optimisation into a Multi Fuel Cell System. In Proceedings of the 2014 IEEE 23rd International Symposium on Industrial Electronics (ISIE), Istanbul, Turkey, 1–4 June 2014; Institute of Electrical and Electronics Engineers (IEEE): Piscataway, NJ, USA, 2014; pp. 218–223.

18. Li, Z.; Zheng, Z.; Xu, L.; Lu, X. A review of the applications of fuel cells in microgrids: Opportunities and challenges. *BMC Energy* **2019**, *1*, 1–23. [CrossRef]

19. Herr, N.; Nicod, J.-M.; Varnier, C.; Jardin, L.; Sorrentino, A.; Hissel, D.; Péra, M.-C. Decision process to manage useful life of multi-stacks fuel cell systems under service constraint. *Renew. Energy* **2017**, *105*, 590–600. [CrossRef]

20. Garcia-Torres, F.; Bordons, C.; Ridao, M.A. Optimal Economic Schedule for a Network of Microgrids With Hybrid Energy Storage System Using Distributed Model Predictive Control. *IEEE Trans. Ind. Electron.* **2018**, *66*, 1919–1929. [CrossRef]

21. Vivas, F.; Segura, F.; Andújar, J.; Caparrós, J. A suitable state-space model for renewable source-based microgrids with hydrogen as backup for the design of energy management systems. *Energy Convers. Manag.* **2020**, *219*, 113053. [CrossRef]

22. Vivas, F.; Heras, A.D.L.; Manzano, F.S.; Andújar, J.M. H2RES2 simulator. A new solution for hydrogen hybridization with renewable energy sources-based systems. *Int. J. Hydrogen Energy* **2017**, *42*, 13510–13531. [CrossRef]

23. Rajalakshmi, N.; Pandiyan, S.; Dhathathreyan, K.S. Design and development of modular fuel cell stacks for various applications. *Int. J. Hydrogen Energy* **2008**, *33*, 449–454. [CrossRef]

24. Vivas, F.; Heras, A.D.L.; Manzano, F.S.; Andújar, J.M. Configuration of a Fuel Cell System. Clues to Choose Between a Modular or Single Stack-Based Design. In Proceedings of the IECON 2016—42nd Annual Conference of the IEEE Industrial Electronics Society, Florence, Italy, 23–26 October 2016; pp. 5466–5472.

25. Bahrami, M.; Martin, J.-P.; Maranzana, G.; Pierfederici, S.; Weber, M.; Meibody-Tabar, F.; Zandi, M. Multi-Stack Lifetime Improvement through Adapted Power Electronic Architecture in a Fuel Cell Hybrid System. *Mathematics* **2020**, *8*, 739. [CrossRef]

26. BALLARD. *FCgen®—1020ACS Fuel Cell Stack Product Manual and Integration Guide*; BALLARD: Seattle, WA, USA, 2011.

27. Vivas, F.J.; Heras, A.D.L.; Manzano, F.S.; Andújar, J.M. Cell voltage monitoring All-in-One. A new low cost solution to perform degradation analysis on air-cooled polymer electrolyte fuel cells. *Int. J. Hydrogen Energy* **2019**, *44*, 12842–12856. [CrossRef]

28. Calderón, A.J.; González, I.; Calderón, M.; Manzano, F.S.; Andújar, J.M. A New, Scalable and Low Cost Multi-Channel Monitoring System for Polymer Electrolyte Fuel Cells. *Sensors* **2016**, *16*, 349. [CrossRef]

29. Prokop, M.; Drakselova, M.; Bouzek, K. Review of the experimental study and prediction of Pt-based catalyst degradation during PEM fuel cell operation. *Curr. Opin. Electrochem.* **2020**, *20*, 20–27. [CrossRef]

30. Chandesris, M.; Médeau, V.; Guillet, N.; Chelghoum, S.; Thoby, D.; Fouda-Onana, F. Membrane degradation in PEM water electrolyzer: Numerical modeling and experimental evidence of the influence of temperature and current density. *Int. J. Hydrogen Energy* **2015**, *40*, 1353–1366. [CrossRef]

31. Petrollese, M.; Isorna, L.V.; Cocco, D.; Cau, G.; Guerra, J. Real-time integration of optimal generation scheduling with MPC for the energy management of a renewable hydrogen-based microgrid. *Appl. Energy* **2016**, *166*, 96–106. [CrossRef]